The Equivalence of Dissipation from Gibbs' Entropy Production with Phase-Volume Loss in Ergodic Heat-Conducting Oscillators

Puneet Kumar Patra, Advanced Technology Development Center
Department of Civil Engineering, Indian Institute of Technology
Kharagpur, West Bengal, India 721302 .
William Graham Hoover and Carol Griswold Hoover
Corresponding Author email : hooverwilliam@yahoo.com
Ruby Valley Research Institute
Highway Contract 60, Box 601, Ruby Valley, Nevada 89833, USA ;
Julien Clinton Sprott, Department of Physics
University of Wisconsin - Madison, Wisconsin 53706, USA ;

(Dated: November 10, 2015)

Abstract

Gibbs' thermodynamic entropy is given by the logarithm of the phase volume, which itself responds to heat transfer to and from thermal reservoirs. We compare the thermodynamic dissipation described by [1] phase-volume loss with [2] heat-transfer entropy production. Their equivalence is documented for computer simulations of the response of an ergodic harmonic oscillator to thermostated temperature gradients. In the simulations one or two thermostat variables control the kinetic energy or the kinetic energy and its fluctuation. All of the motion equations are time-reversible. We consider both *strong* and *weak* control variables. *In every case the time-averaged dissipative loss of phase-space volume coincides with the entropy produced by heat transfer.* Linear-response theory nicely reproduces the small-gradient results obtained by computer simulation. The thermostats considered here are *ergodic* and provide simple dynamical models, some of them with as few as *three* ordinary differential equations, while remaining capable of reproducing Gibbs' canonical phase-space distribution and precisely consistent with irreversible thermodynamics.

Keywords: Ergodicity, Algorithms, Entropy Production, Dissipation

I. INTRODUCTION

We discuss the time-reversibility and thermodynamic dissipation of several harmonic-oscillator models, all of them *extensions* of the thermostated canonical-ensemble dynamics pioneered by Shuichi Nosé in 1984[1,2]. All the resulting extended models[3–13] studied here are chaotic and ergodic. They generate phase-space distributions matching Gibbs' canonical distribution, Gaussian in the oscillator coordinate q and momentum p with halfwidths corresponding to the kinetic temperature T .

Our *nonequilibrium* extensions of these equilibrium models result when the thermostat temperature has a spatial gradient with $T = T(q)$. All such nonequilibrium models discussed here generate heat flows obeying the Second Law of Thermodynamics. All these nonequilibrium models generate *fractal* rather than smooth phase-space distributions. The fractals' time dependence chronicles the penetration of the fractal character to smaller and smaller length scales with passing time, and is fully consistent with Gibbs' phase-volume definition of entropy.

We begin with a brief discussion of time reversibility and ergodicity in Section II. Section III provides a historical sketch of time-reversible thermostat models from Nosé's work to the present. Section IV illustrates the time-reversibility of the models in nonequililbrium stationary flows and demonstrates the consistency of all the thermostat models with Gibbs' statistical thermodynamics. Section V illustrates the consistency of these steady flows with Green and Kubo's treatment of near-equilibrium linear-response theory. We consider the details of the linear-response approach for two models[7,11]. Our Summary and Historical Perspective Section VI includes our main conclusion from this work: useful computational thermostats can be and should be chosen so that the thermodynamic dissipation away from equilibrium is consistent with the Second Law of Thermodynamics where the entropy corresponds to Gibbs' phase-volume definition. We relate this finding to the history of understanding microscopic systems through the computational study of small-system dynamics.

II. TIME-REVERSIBLE ERGODICITY AT AND AWAY FROM EQUILIBRIUM

Thirty years ago Nosé and Hoover developed two new mechanics formally consistent with Gibbs' canonical ensemble[1–4]. These modern mechanics share two fundamental char-

acteristics of their Hamiltonian ancestor, being both deterministic and *time-reversible*. Any sequence of successive frames of a Nosé or Nosé-Hoover movie played "backward", with the frames in reversed order, shows a reversed motion described by exactly the same motion equations but with reversed velocities. Hamiltonian mechanics shares this same time-reversibility property.

The harmonic oscillator provides the simplest example of reversibility. If we choose a harmonic oscillator with unit mass and spring constant any "forward" orbit (with $-\tau < t < +\tau$) can be paired with a time-reversed backward twin with the reversal occurring at time $t = 0$. For instance :

$$\{ \; q = \pm \sin(t) \; ; \; p = \pm \cos(t) \; \} \longleftrightarrow \{ \; q = \mp \sin(t) \; ; \; p = \mp \cos(t) \; \} \; .$$

Both orbits satisfy Hamilton's equations $\{ \; \dot{q} = +p \; ; \; \dot{p} = -q \; \}$. In this simplest case the reversed version is also a mirror image of the original, with both q and p changed in sign. In both cases, forward and backward, time *increases*. This corresponds to a positive timestep $dt > 0$ in a numerical simulation. We distinguish this physical version of "time reversibility" from its mathematical cousin where dt changes sign while q and p do not.

Nosé sought out a dynamics which would explore the (q, p) phase space with a probability density approaching Gibbs' canonical distribution, $f(q, p) \propto e^{-\mathcal{H}(q,p)/kT}$. Both the Nosé and the simpler Nosé-Hoover thermostat algorithms lacked the ergodicity required to reproduce all of Gibbs' canonical distribution for the prototypical one-dimensional harmonic oscillator[3]. About a decade later three more-complex algorithms, *doubly-thermostated* with four motion equations rather than singly-thermostated with three, were developed. All three have been shown to provide ergodicity for the oscillator[5–8]. How is this ergodicity demonstrated ?

First of all ergodic motion equations necessarily satisfy the *stationary* version of Liouville's continuity equation :

$$(\partial f / \partial t) = -\nabla_r \cdot (f v) \equiv 0 \; .$$

Abbreviate the Nosé-Hoover motion equations for an oscillator by a introducing a generalized velocity v for the three-dimensional flow :

$$v = \dot{r} = (\dot{q}, \dot{p}, \dot{\zeta}) \longleftarrow \{ \; \dot{q} = +p \; ; \; \dot{p} = -q - \zeta p \; ; \; \dot{\zeta} = (p^2/T) - 1 \; \} \; [\; \mathrm{NH} \;] \; ,$$

where the stationary distribution f is proportional to $e^{-q^2/2T} e^{-p^2/2T} e^{-\zeta^2/2}$. The four non-

vanishing contributions to $(\partial f/\partial t)$ are :

$$-\dot{q}(\partial f/\partial q) = p(q/T)f \ ; \ -\dot{p}(\partial f/\partial p) = (-q - \zeta p)(p/T)f \ ;$$

$$-\dot{\zeta}(\partial f/\partial \zeta) = [\ (p^2/T) - 1\ ](\zeta)f \ ; \ -f(\partial \dot{p}/\partial p) = f\zeta \ .$$

These four terms do sum to zero, showing that the motion equations are consistent with the assumed Gaussian distribution. The Nosé-Hoover equations are *not* ergodic so that the vanishing of $(\partial f/\partial t)$ is not *sufficient* for ergodicity. In fact, numerical work shows that only a bit less than six percent of the Gaussian oscillator measure is mixing and chaotic. The remaining 94 percent is made up of regular tori, showing that the Nosé-Hoover distribution is not ergodic. See **Figure 1** for a cross-sectional view of the Nosé-Hoover oscillator's chaotic sea.

We use the term "chaotic" in the usual sense here, to indicate that the maximum Lyapunov exponent has a longtime positive average value. Numerical methods for measuring Lyapunov exponents so as to characterize chaos make up a vast literature readily accessible through Wikipedia.

Ergodic motion equations must necessarily reproduce the canonical moments of the Maxwell-Boltzmann velocity distribution. With mkT chosen equal to unity to set the temperature scale, the values appropriate for Cartesian coordinates ,

$$\langle\ p^{2,4,6,\cdots}\ \rangle_{MB} = 1, 3, 15, \ldots$$

can readily be verified from numerical simulations. But distributions which are "almost" ergodic (for some specific æsthetic examples see Figures 2-4 in Reference 13) can exhibit deviations so small as to be masked by thermal fluctuations.

Two better checks of ergodicity have been implemented. Cross sections [such as the $(q, p, 0)$ points shown in **Figure 1**], where $\zeta = 0$ or where $\zeta = \xi = 0$ if two thermostat variables are used can be inspected visually for the tell-tale holes indicating regular toroidal solutions within the chaotic sea.

Additionally, the mean value of the largest Lyapunov exponent λ_1 (the longtime averaged rate of separation of two nearby trajectories, positive for chaos and zero for tori) can be estimated for simulations using millions or billions of randomly chosen initial conditions. For an *ergodic* system the results cluster around a unique positive longtime average, $\langle\ \lambda_1(t)\ \rangle \simeq \lambda_1$. For a toroidal system the averaged results instead cluster about zero.

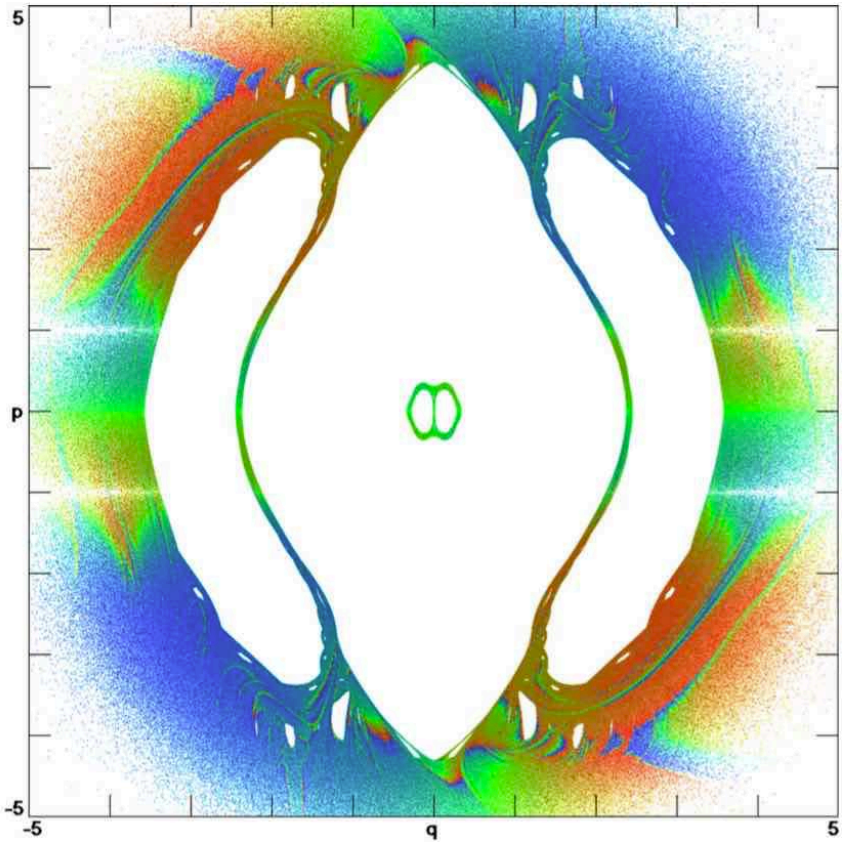

FIG. 1: Penetrations of the $(q, p, 0)$ plane for the chaotic Nosé-Hoover oscillator with initial condition $(0, 5, 0)$, using points from an adaptive fourth-order Runge-Kutta integration with a timestep $dt \simeq 0.001$. Red and blue correspond to the most positive and most negative Lyapunov exponents. Notice the lack of symmetry about the horizontal axis despite the time-reversibility of the equations of motion, showing that the Lyapunov exponents' dependence on past history differs from their relation to the unforseeable future. This cross section of the chaotic sea corresponds to about six percent of the Nosé-Hoover oscillator's Gaussian measure. Note the mirror-image inversion symmetry.

The three criteria [moments, tell-tale holes, Lyapunov exponent] have been applied to the thermostats described in the following Section leading to the conclusion that many different one-thermostat and two-thermostat systems *are* ergodic. Let us detail four such systems next.

III. DETERMINISTIC TIME-REVERSIBLE THERMOSTATS (1984-2015)

As recently as early 2015 it was thought that four or more ordinary differential equations were required for oscillator ergodicity. Reference 8 deals with techniques for demonstrating ergodicity as applied to the Martyna-Klein-Tuckerman[5], Ju-Bulgac[6], and Hoover-Holian[7] thermostated oscillators. For a more comprehensive treatment see References 9 and 10. The three thermostat types, MKT, JB, and HH, produce chaotic dynamics $(\dot{q}, \dot{p}, \dot{\zeta}, \dot{\xi})$ which pass visual ergodicity tests. All three of them also closely reproduce the Cartesian velocity moments $\langle\ p^{2,4,6}\ \rangle$ characterizing the equilibrium Maxwell-Boltzmann distribution. Let us begin by reviewing the structure of these three thermostat types.

A. The Martyna-Klein-Tuckerman "Chain" Thermostat (1992)

The Martyna-Klein-Tuckerman thermostat uses two control variables, ζ and ξ, with ζ controlling $\langle\ p^2\ \rangle$ and ξ controlling $\langle\ \zeta^2\ \rangle$:

$$\{\ \dot{q} = p\ ;\ \dot{p} = -q - \zeta p\ ;\ \dot{\zeta} = (p^2/T) - 1 - \xi\zeta\ ;\ \dot{\xi} = \zeta^2 - 1\ \}\ [\ \mathrm{MKT}\ ]\ .$$

The steady-state distribution corresponding to these oscillator motion equations is an extension of Gibbs' canonical one :

$$f_{\mathrm{MKT}}(q,p,\zeta,\xi) \propto e^{-q^2/2T} e^{-p^2/2T} e^{-\zeta^2/2} e^{-\xi^2/2} \longrightarrow$$

$$(\partial f/\partial t) = -\nabla_r \cdot (fv) \equiv 0 \text{ where } v = \dot{r} \equiv (\dot{q}, \dot{p}, \dot{\zeta}, \dot{\xi})\ .$$

The *stationarity* test from the continuity equation, $(\partial f/\partial t) = 0$, provides a necessary, but not necessarily sufficient, condition that *any* set of motion equations must satisfy for ergodicity. Martyna, Klein, and Tuckerman[5] emphasized that any number of additional control variables can be added to form a "chain" of thermostats.

B. The Ju-Bulgac Cubic Thermostat (1993)

The Ju-Bulgac thermostat[6] likewise uses two control variables but includes *cubic* dependences following the observation of Bauer, Bulgac, and Kusnezov that cubic terms enhance chaos and ergodicity[6,9,10] :

$$\{\ \dot{q} = p\ ;\ \dot{p} = -q - \zeta^3 p - \xi(p^3/T)\ ;\ \dot{\zeta} = (p^2/T) - 1\ ;\ \dot{\xi} = (p^4/T^2) - 3(p^2/T)\ \}\ [\ \mathrm{JB}\ ]\ .$$

The steady-state distribution here is Gaussian in ζ^2 rather than ζ :

$$f_{\rm JB}(q,p,\zeta,\xi) \propto e^{-q^2/2T} e^{-p^2/2T} e^{-\zeta^4/4} e^{-\xi^2/2} \longrightarrow (\partial f/\partial t) \equiv 0.$$

At unit temperature $T = 1$ the rms rate $\mid \dot{p} \mid$ at which the Ju-Bulgac momentum moves through phase space is about three times faster than that of the simpler Martyna-Klein-Tuckerman momentum :

$$\sqrt{\langle\ q^2 + p^2\zeta^6 + p^6\xi^2\ \rangle} \simeq \sqrt{18.028}\ versus\ \sqrt{\langle\ q^2 + p^2\zeta^2\ \rangle} = \sqrt{2}\ .$$

From the numerical standpoint cubic thermostat variables enhance chaos and mixing without incurring the considerable stiffness associated with quintic controls.

C. The Hoover-Holian Thermostat (1996)

Like the two preceding, the Hoover-Holian thermostat[7] uses two control variables. The first one is allocated to fixing the oscillator temperature $\zeta \rightarrow \langle\ p^2\ \rangle$ while the second fixes the fluctuation of the temperature $\xi \rightarrow \langle\ p^4\ \rangle$:

$$\{\ \dot{q} = p\ ;\ \dot{p} = -q - \zeta p - \xi(p^3/T)\ ;\ \dot{\zeta} = (p^2/T) - 1\ ;\ \dot{\xi} = (p^4/T^2) - 3(p^2/T)\ [\ \text{HH}\ ]\ .$$

At unit temperature the rms rate at which the Hoover-Holian momentum moves, $\sqrt{\langle\ q^2 + p^2\zeta^2 + \xi^2 p^6\ \rangle} = \sqrt{17}$, is nearly the same as the Ju-Bulgac speed. The Hoover-Holian thermostat variables ζ and ξ exert what we term "strong" control of the temperature and its fluctuation, in that longtime averages of the thermostat motion equations constrain moments proportional to the kinetic energy and its fluctuation :

$$\langle\ \dot{\zeta}\ \rangle = 0 \longrightarrow \langle\ (p^2/T)\ \rangle \equiv 1\ ; \langle\ \dot{\xi}\ \rangle = 0 \longrightarrow \langle\ (p^4/T^2)\ \rangle \equiv \langle\ 3(p^2/T)\ \rangle\ .$$

These strong constraints can be applied equally well in nonequilibrium situations. Nonequilibrium applications of the MKT thermostat typically lead to nonzero correlated values of the thermostat variables, $\langle\ \zeta\xi\ \rangle$ so that the definition of the kinetic temperature $\langle\ (p^2/T)\ \rangle \equiv 1$ is violated.

At equilibrium the steady-state distribution corresponding to the HH motion equations is exactly the same as the Martyna-Klein-Tuckerman four-dimensional Gaussian :

$$f_{\rm HH}(q,p,\zeta,\xi) = f_{\rm MKT}(q,p,\zeta,\xi) \propto e^{-q^2/2T} e^{-p^2/2T} e^{-\zeta^2/2} e^{-\xi^2/2} \longrightarrow (\partial f/\partial t) \equiv 0\ .$$

D. The Ergodic Single-Thermostat 0532 Model (2015)

Very recently[11–13] a variety, both novel and wide, of *singly*-thermostated ergodic algorithms has been developed and applied to the one-dimensional harmonic oscillator. The simplest of them, the "0532 Model", consists of only three ordinary differential equations for the oscillator coordinate q , velocity p , and friction coefficient ζ at a thermostat temperature T :

$$\dot{q} = p \ ; \ \dot{p} = -q - \zeta[\ 0.05p + 0.32(p^3/T) \ ] \ ;$$

$$\dot{\zeta} = 0.05[\ (p^2/T) - 1 \ ] + 0.32[\ (p^4/T^2) - 3(p^2/T) \ ] \ ; \ [\ 0532 \text{ Model }] \ .$$

We term this simultaneous control of the second and fourth moments, $\langle \ p^{2 \text{ and } 4} \ \rangle$, "weak" because a linear combination of the moments is controlled rather than enforcing the separate control of *both* moments, as in the earlier work in References 5-9 . Numerical solutions of the 0532 oscillator model indicate that it *is* ergodic and corresponds to Gibbs' canonical ensemble multiplied by a Gaussian distribution for the thermostat control variable ζ :

$$f_{0532}(q,p,\zeta,\xi) =\propto e^{-q^2/2T} e^{-p^2/2T} e^{-\zeta^2/2} \longrightarrow (\partial f/\partial t) \equiv 0 \ .$$

Because the 0532 model motion occurs in just three dimensions rather than four, it is well-suited to analysis. This model, like its three predecessors in this Section, is time-reversible, even in the nonequilibrium case where the temperature varies in space, $T = T(q)$. Let us review the reversibility property in that specific *nonequilibrium* case.

IV. TIME REVERSIBILITY AWAY FROM EQUILIBRIUM – 0532 MODEL

At equilibrium the forward and backward trajectories for canonical oscillators, using any of the four ergodic sets of motion equations, are qualitatively much the same. No holes in the cross sections, good values for the even velocity moments, longtime averaged Lyapunov exponent the same for any initial condition. In short – deterministic, time-reversible, ergodic.

Away from equilibrium, thermodynamic dissipation can be investigated, still time-reversibly, by adding a localized temperature gradient $(dT/dq) = [\ \epsilon/\cosh^2(q) \ ]$ enabling heat transfer through a nonzero average current $(p^3/2)$:

$$1 - \epsilon < T < 1 + \epsilon = T(q) = 1 + \epsilon \tanh(q) \longrightarrow \langle \ (p^3/2) \ \rangle < 0 \longrightarrow (\dot{S}/k) < 0 \ .$$

Here ϵ is the maximum value of the temperature gradient, $T'(0)$. The negative entropy change, causing the phase volume to shrink onto a strange attractor is due to the net heat loss *from* the oscillator *to* the coordinate-dependent 0532 thermostat temperature $T(q)$. From the standpoint of steady-state irreversible thermodynamics the overall heat loss is offset by an internal "entropy production" so that the *net* change of oscillator "entropy" vanishes. We remind the reader that Gibbs' entropy is minus infinity for fractal attractors so that the irreversible-thermodynamics concept of nonequilibrium entropy is problematic. The artificial entropy change could be also be viewed as the result of ongoing coarse-graining (which would artificially increase Gibbs' entropy) at the level of the computational roundoff error (in the sixteenth or seventeenth digit).

The temperature gradient destroys the "global [overall] reversibility" of the motion equations. Although in principle reversible the chaotic instability of the dynamics, evidenced by a positive Lyapunov exponent, makes this "irreversibility" possible. This irreversibility is evidenced by a Lyapunov spectrum with a *negative* sum so that the longtime averaged distribution is a fractal strange attractor with a reduced information dimension rather than a smooth three-dimensional Gibbsian distribution.

Among the thermostats we have considered only the Nosé-Hoover equations show that a fractal attractor is *not* inevitable. In the Nosé-Hoover case a majority of initial conditions give rise to phase-space tori, orbits with no longtime tendency toward dissipation. All of the ergodic thermostats invariably produce small-gradient dissipation rather than tori so that their orbits exhibit what we call "global irreversibility".

The equilibrium ($\epsilon = 0$ and unit temperature $T = 1$) Lyapunov spectrum for the 0532 model, $\{ +0.144, 0, -0.144 \}$ sums to zero corresponding to the three-dimensional Gaussian distribution, $f \propto e^{-q^2/2} e^{-p^2/2} e^{-\zeta^2/2}$. The time-averaged growth rates of infinitesimal one-, two-, and three-dimensional phase space volumes are given by

$$\{ \lambda_1,\ \lambda_1 + \lambda_2,\ \lambda_1 + \lambda_2 + \lambda_3 \} .$$

In the nonequilibrium case with $\epsilon = 0.50$ the time-averaged spectrum becomes asymmetric, $\{ +0.1135, 0, -0.1454 \}$, corresponding to the time-averaged growth of a length or an area in phase space $\simeq e^{+0.1135t}$ but to *shrinkage* of an infinitesimal three-dimensional phase volume $\otimes$:

$$(\dot{\otimes}/\otimes) = 0.1135 - 0.1454 = -0.0319 \longrightarrow D_{KY} = 2 + (0.1135/0.1454) = 2.78 .$$

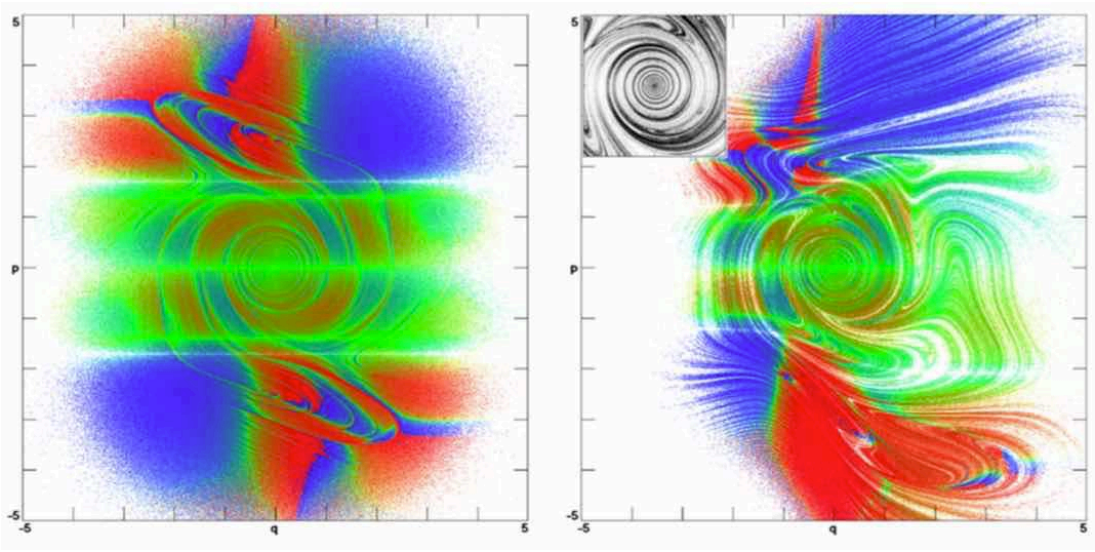

FIG. 2: Penetrations of the $(q, p, 0)$ plane for the chaotic and ergodic 0532 Model using adaptive fourth-order Runge-Kutta integration with a timestep $dt \simeq 0.001$. The red and blue points correspond to maximum and minimum values of the local Lyapunov exponent. The equilibrium $\zeta = 0$ cross section at the left shows inversion symmetry, corresponding to viewing the oscillator in a mirror. The lack of symmetry about the horizonal $p = 0$ axis shows that the exponents depend upon the past rather than the future. The nonequilibrium section ($\epsilon = 0.50$) shown to the right displays no symmetry and is multifractal. The black-and-white inset shows the cross-sectional density in the 2×2 central region of the phase-plane section.

Kaplan and Yorke's linear interpolation predicts a strange-attractor dimension of 2.78. Cross sections of the equilibrium and nonequilibrium 0532 dynamics are shown in **Figure 2** . Just as at equilibrium the nonequilibrium strange-attractor's motion equations are time-reversible. Any forward-in-time sequence $\{ +q, +p, +\zeta \}$ corresponds to a twin sequence $\{ +q, -p, -\zeta \}$ with the order of the (q, p, ζ) points reversed. *Locally* this reversed sequence satisfies the same equations of motion with errors of order $(dt^5/120)$ for fourth-order

Runge-Kutta integration. But any attempt to *generate* such a reversed sequence numerically fails because the Lyapunov spectrum of the reversed sequence would correspond to $\{ +0.1454, 0, -0.1135 \}$. The positive exponent sum indicates an unstable *repellor* with a *diverging* phase volume, $(\dot{\otimes}/\otimes) = +0.0319$. Any attempt to follow the repellor numerically will instead seek out the nearby attractor (both are still ergodic, at least if ϵ is small) which, though unstable for a line or an area, is less so than the repellor. The repellor properties *can* (only) be observed by the expedient of *storing* and reversing a trajectory. The cross section associated with a stored ten-billion-point attractor trajectory is illustrated in **Figure 3** . Note the lack of $\pm p$ symmetry in the coloring of the local Lyapunov exponent, $\lambda_1(t)$.

This instructive problem illustrates two general principles : [1] the phase volume of the steady-state attractor is zero and singular everywhere *despite the time-reversibility of the motion equations* ; [2] any typical three-dimensional phase volume first expands and leaves the vicinity of the (ergodic) fractal repellor and then shrinks in order to join its mirror-image (and likewise ergodic) fractal attractor exponentially fast. Both these features correspond to the paucity of nonequilibrium states and to the irreversibility described by the Second Law of Thermodynamics.

There is more. Consider two additional equally-significant observations. First, the comoving shrinkage rate in phase space corresponds precisely and instantaneously to the loss of Gibbs' entropy for the system. To illustrate consider the 0532 model ,

$$\dot{q} = p \ ; \ \dot{p} = -q - \zeta[\ 0.05p + 0.32(p^3/T) \ ] \ [\ 0532 \ ] \ .$$

$$(\dot{S}/k) = (\dot{\otimes}/\otimes) \equiv (\partial\dot{q}/\partial q) + (\partial\dot{p}/\partial p) + (\partial\dot{\zeta}/\partial\zeta) = 0 - \zeta[\ 0.05 + 0.96(p^2/T) \ ] + 0 \ .$$

Second, this loss rate also corresponds precisely, *when time-averaged*, to the kinetic energy (or heat Q) extracted by the thermostat forces, divided by the thermostat temperature T :

$$\langle \ (\dot{Q}/T) \ \rangle = -\langle \ \zeta[\ 0.05(p^2/T) + 0.32(p^4/T^2) \ ] \ \rangle = \langle \ (\dot{S}/k) \ \rangle \ .$$

The time-averaged value $\langle \ \zeta[\ 0.05 + 0.96(p^2/T) \ ] \ \rangle$, follows from the time-averaged evolution equation for the squared thermostat variable $(\zeta^2/2)$:

$$\langle \ \zeta\dot{\zeta} = 0 = 0.05\zeta[\ (p^2/T) - 1 \ ] + 0.32\zeta[\ (p^4/T^2) - 3(p^2/T) \ ] \ \rangle \ .$$

The time-averaged phase-volume loss, equivalent to the dissipation seen in the heat Q lost to thermal reservoirs divided by the reservoir temperature T ,

$$\langle \ (\dot{Q}/T) \ \rangle = \langle \ k(\dot{\otimes}/\otimes) \ \rangle = \langle \ \dot{S} \ \rangle \ ,$$

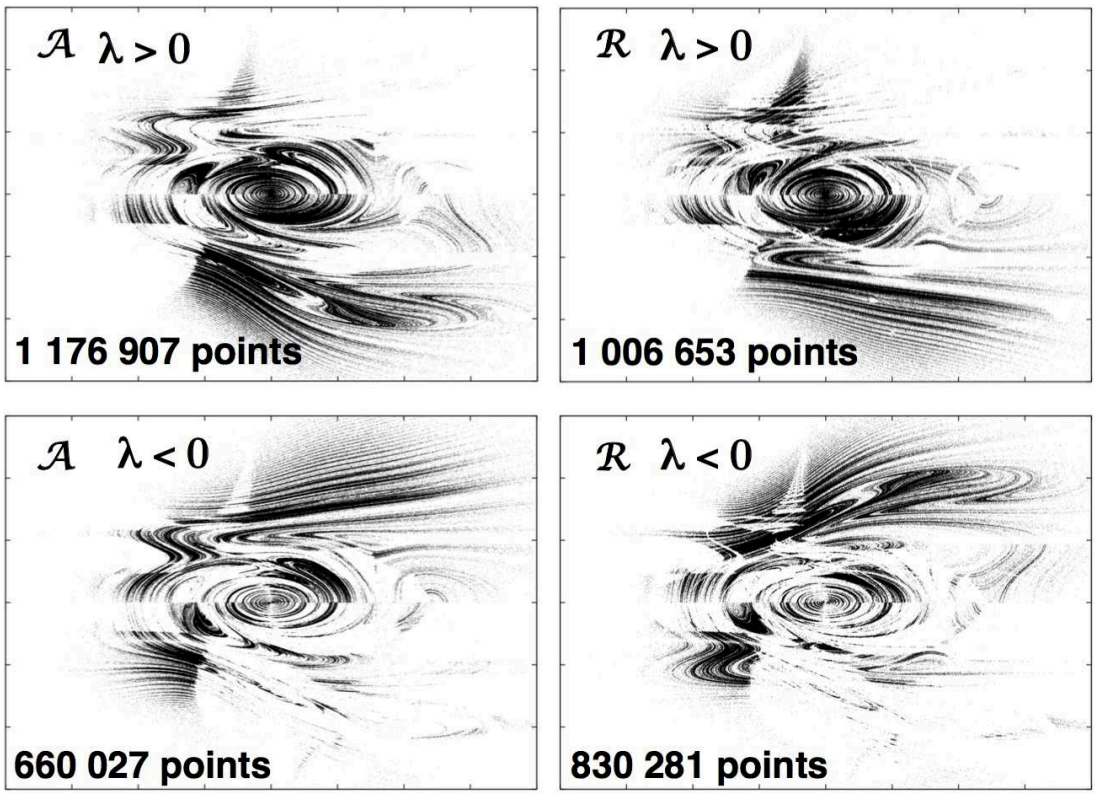

FIG. 3: Penetrations of the $(q, p, 0)$ plane for the chaotic and ergodic 0532 Model using a ten-billion-point attractor reference trajectory (denoted A) and classic fourth-order Runge-Kutta integration with a timestep $dt = 0.001$ for the satellite trajectory. This chaotic trajectory crosses the $\zeta = 0$ plane 1 836 934 times. The signs of the largest Lyapunov exponent at each crossing are indicated for both the attractor and the repellor (denoted R). By plotting the positive and negative points separately the lack of any symmetry is clear. The repellor points are identical to those of the attractor but are traced out in the opposite direction. For both the attractor and the repellor the separation of the reference and satellite trajectories is $\sqrt{(q_s - q_r)^2 + (p_s - p_r)^2 + (\zeta_s - \zeta_r)^2} = 0.000001$. The $p(q)$ region shown is $\mid q \mid < 4$; $\mid p \mid < 6$.

holds generally for *all* the thermostat models discussed here. This identity holds even for the Nosé-Hoover model, which is not ergodic. It holds for other power laws. Suppose for instance that the thermostat force is proportional to odd powers of ζ and p :

$$-A_{mn}\zeta^{2m+1}(p^{2n+1}/T^n)$$

so that the equilibrium distribution is proportional to

$$f \propto e^{-p^2/2T} e^{-\zeta^{2m+2}/(2m+2)} \ .$$

Gibbs' phase-space dissipation, from $-(\partial \dot{p}/\partial p)$ gives a contribution to the system entropy :

$$(\dot{S}/k) = -(2n+1) A_{mn} \zeta^{2m+1} (p^{2n}/T^n)$$

The entropy change from the contribution of the same dissipative term to heat transfer is :

$$(\dot{Q}/T) = -A_{mn} \zeta^{2m+1} (p^{2n+2}/T^{n+1}) \ .$$

A look at the equation of motion for the friction coefficient, multiplied by ζ^{2m+1} and time averaged shows that $(\dot{S}/k)$ and $(\dot{Q}/T)$ are equivalent :

$$\langle \ \zeta^{2m+1} \dot{\zeta} \ \rangle = \langle \ \zeta^{2m+1} A_{mn} [\ (p^{2n+2}/T^{n+1}) - (2n+1)(p^{2n}/T^n) \ ] \ \rangle = 0,$$

This is a consequence of the vanishing of the longtime averaged value of a bounded quantity, in this case $(d/dt)[\ \zeta^{2m+2}/(2m+2) \ ]$. Generalized models, like the 0532 model, can use two or more power-law contributions to thermostat forces. This equivalence of Gibbs' entropy production with that from irreversible thermodynamics points the way forward toward consistent theories of nonequilibrium steady states either near to or far from equilibrium.

In the past it has been pointed out that it *is* possible to develop thermostats for which the phase-volume and heat-transfer rates are *not* closely related[15–17]. This potential loss of a family relationship recalls Tolstoy's thought: "All happy families are alike ; each unhappy family is unhappy in its own way." We emphasize here that the close relationship linking phase volume to thermodynamics is to be celebrated rather than avoided.

We note that our dimensionless friction coefficients *could* be multiplied by relaxation times or by powers of the temperature, changing their units. We have carefully chosen the forms used here in order to guarantee the consistency of the motion equations with both Gibbs' canonical distribution and with thermodynamics. Dimensionless friction coefficients seem to us the simplest approach to thermodynamic consistency.

In the 1950s Green and Kubo showed that their "linear-response" theory expresses nonequilibrium transport coefficients in terms of equilibrium correlation functions. This same theory can be applied to the various thermostats we have described. Next we illustrate this idea for two examples, the doubly-thermostated Hoover-Holian thermostat and the singly-thermostated 0532 Model.

V. LINEAR RESPONSE THEORY WITH A TEMPERATURE GRADIENT

We have celebrated the equivalence of two measures of dissipation, phase volume loss and Gibbs' entropy production when any one of our five of thermostat models [NH, MKT, JB, HH, 0532] is time averaged. This equivalence guarantees their usefulness in simulations consistent with dynamical equivalents of the canonical ensemble. Green-Kubo linear-response theory is a perturbation theory based on Gibbs' ensembles. Typically the energy is modified by a perturbation, giving rise to a nonequilibrium flux. In our case both the energy and the temperature are modified by introducing a temperature profile along with a stabilizing frictional force. Let us demonstrate their theory's usefulness for the Hoover-Holian (q, p, ζ, ξ) and the 0532 Model (q, p, ζ) oscillators as two concrete examples.

A. Hoover-Holian Oscillator with Temperature Gradient

We begin with the extended canonical distribution for the oscillator with energy E and at a temperature T of unity :

$$f(q,p,\zeta,\xi)_{\rm HH} \propto e^{-\mathcal{H}(q,p)/kT} e^{-\zeta^2/2} e^{-\xi^2/2} = e^{-q^2/2T} e^{-p^2/2T} e^{-\zeta^2/2} e^{-\xi^2/2} \ .$$

Adding a temperature perturbation ,

$$T = 1 \longrightarrow T = 1 + \Delta T = 1 + \epsilon \tanh(q) \ ,$$

we wish to compute the responding current, $(p^3/2)$ as a function of time.

The simplest form of the Hoover-Holian motion equations is :

$$\{ \ \dot{q} = p \ ; \ \dot{p} = -q - \zeta p - \xi(p^3/T) \ ; \ \dot{\zeta} = (p^2/T) - 1 \ ; \ \dot{\xi} = (p^4/T^2) - 3(p^2/T) \ \} \ [\ {\rm HH} \ ] \ .$$

The time-dependent change of the canonical weight $e^{-\Delta(E/kT)}$ can be linearized in the thermal perturbation ϵ with the result :

$$(f_{neq}/f_{eq}) = 1 + \int_0^t [\ \epsilon \tanh(q) \ ]_0[\ -\zeta p^2 - \xi(p^4/T) \ ]_{t'} dt' \ .$$

We can use this *nonequilibrium* perturbation to compute the current $(p^3/2)$ at time t from the *equilibrium* correlation function (which depends only on the time difference t') :

$$\langle \ (p^3/2) \ \rangle_{\rm neq} = \int_0^t \langle \ [\ \epsilon \tanh(q) \ ]_0[\ -\zeta p^2 - \xi(p^4/T) \ ]_0 (p^3/2)_{t'} \ \rangle_{\rm eq} dt' \ .$$

A highly-accurate equilibrium calculation can be based on the fact that the four-dimensional equilibrium measure is ergodic, a Gaussian probability density known in advance. To compute averages we begin with a grid of [$100 \times 100 \times 100 \times 100$] equiprobable points and use these as the initial conditions for computing both the nonequilibrium current and the equilibrium correlation function. The excellent agreement shown in **Figure 4** confirms the analysis showing that both the equilibrium distribution function and its linear perturbation are well suited to numerical exploration. The figure compares the linear-response expression for the current to that actually measured with nonequilibrium molecular dynamics at the relatively small field strength $\epsilon = 0.10$. We conclude that simple linear-response theory is a fringe benefit of our deterministic ergodic thermostat models.

The 0532 Model has only three phase-space dimensions rather than four so that the linear response simulation is about three orders of magnitude, one thousand times, faster. The agreement between the linear-response and directly measured current is likewise excellent, as is shown in **Figure 5**. Evidently the ergodic thermostats reproduce both Gibbs' canonical distribution and linear nonequilibrium perturbations as described by Green-Kubo theory.

VI. SUMMARY AND HISTORICAL PERSPECTIVE

A wide variety of time-reversible thermostats all generate Gibbs' canonical ensemble through deterministic chaos. When the kinetic temperature varies with coordinate, the resulting heat current $(p^3/2)$ leads to dissipation, heat transfer, and entropy change. The steady loss of comoving phase volume obeys Gibbs' thermodynamic relations in the extended phase space :

$$\langle\ (\dot{S}/k) = (\dot{Q}/kT) = (\dot{\otimes}/\otimes)\ \rangle\ ,$$

where the comoving phase volume includes extensions in the thermostat directions. These time-averaged relations hold even for the nonergodic Nosé-Hoover oscillator :

$$\langle\ (\dot{\otimes}/\otimes)\ \rangle = -\langle\ \zeta\ \rangle = -\langle\ \zeta(p^2/T)\ \rangle = \langle\ (\dot{S}/k)\ \rangle\ [\ \mathrm{NH}\ ]\ .$$

Because the ergodic thermostats all generate Gibbs' canonical distribution they also give linear-response relations linking the nonequilibrium currents and thermal gradients. We believe that these observations are fundamental to a systematic exploration of nonequilibrium

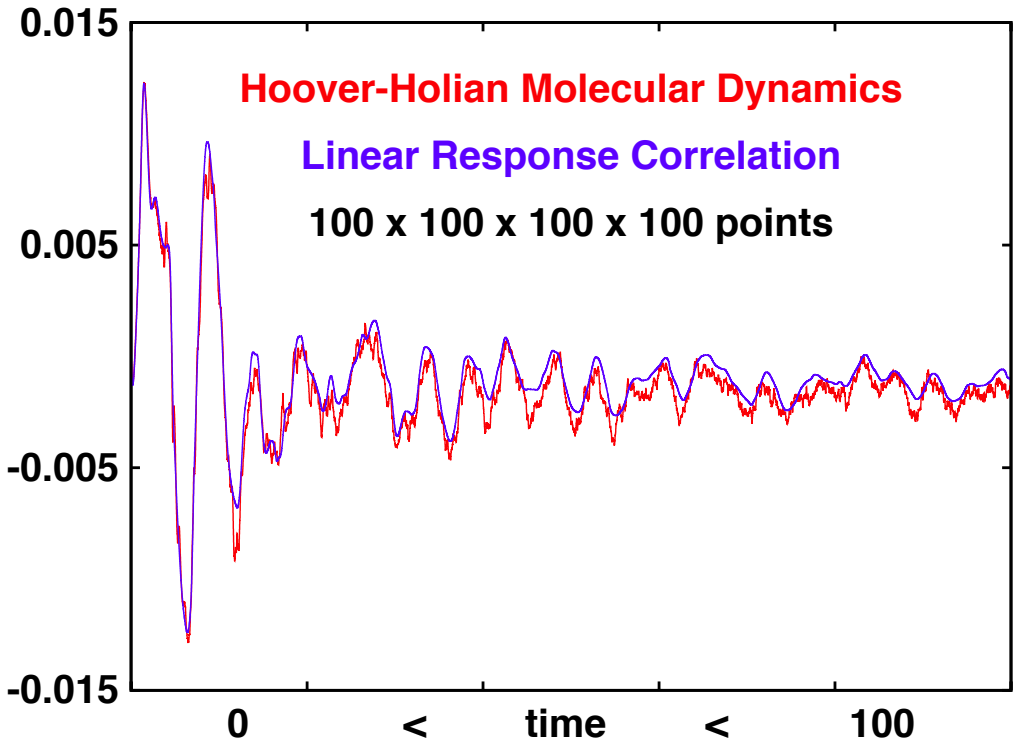

FIG. 4: Comparison of the linear-response correlation integral (blue) with the measured current (red) for the HH oscillator at a field strength $\epsilon = 0.10$. Results for $T = 1 + 0.10\tanh(q)$ (shown here) and $T = [\ 1 - 0.10\tanh(q)\ ]^{-1}$ are very similar and confirm that $\epsilon = 0.10$ is close to the linear regime. The phase-space integration uses 100^4 equally-probable Gaussian points as the initial states for the averaged current $\langle\ (p^3/2)\ \rangle$ and for the linear-response correlation integral.

statistical mechanics through thermostated dynamics.

Our presentday understanding of nonequilibrium systems has its basis in the work of Boltzmann, the Ehrenfests, Gibbs, and Maxwell. 50 years of numerical work have provided alternatives to their classic Hamiltonian and stochastic models. Deterministic reproducibility with dissipative time-reversibility have provided explicit links between microscopic nonequilibrium molecular dynamics and macroscopic thermodynamics.

Shockwave studies which generate localized far-from-equilibrium states would seem to be an ideal problem for consolidating these gains in understanding. Shock dynamics *is*

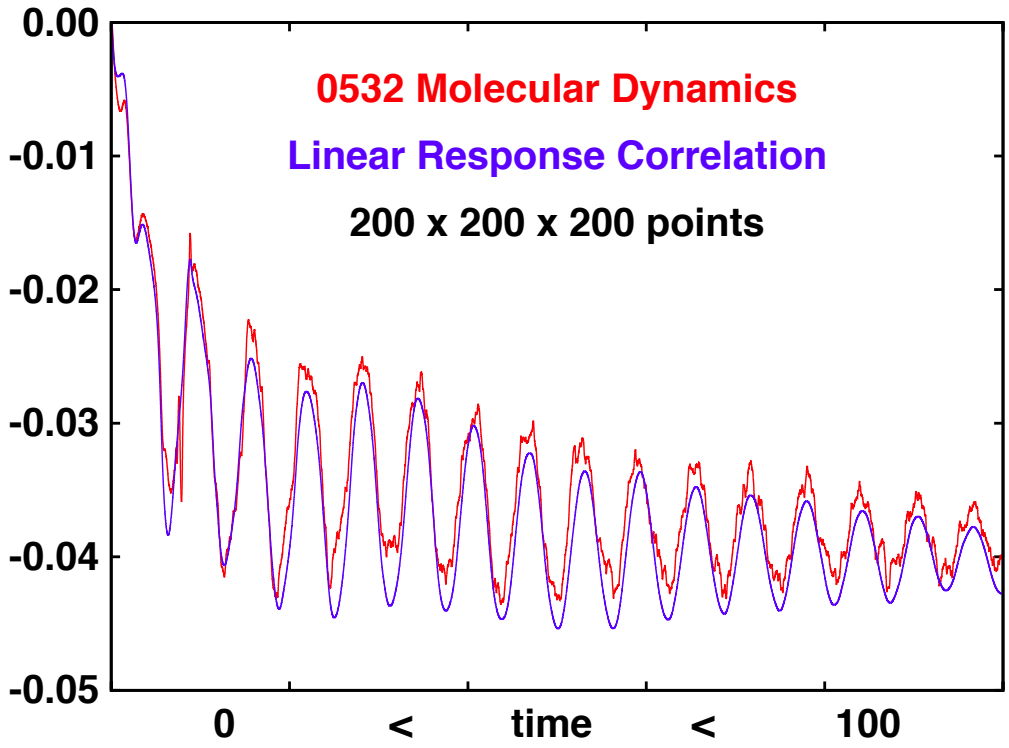

FIG. 5: Comparison of the linear-response correlation integral with the measured current for the 0532 oscillator at a field strength $\epsilon = 0.10$. We show results for $T = 1 + 0.10\tanh(q)$ which closely resemble those for $T = [\ 1 - 0.10\tanh(q)\ ]^{-1}$ confirming that $\epsilon = 0.10$ is close to the linear regime. The three-dimensional Gaussian phase-space integration uses 200^3 equally-probable points as the initial states for both the average current and the correlation integral.

purely Hamiltonian inside the wave and with equilibrium cold and hot boundaries. The relaxation times correspond to vibrational collision times. The nonlinear dependence of transport coefficients and the irreversible nature of the timelag between forces and fluxes can be measured directly in shockwaves[18]. There is a comprehensive listing of nearly all the existing approaches to nonequilibrium systems in Jepps and Rondoni's review[19]. This variety illustrates that many tools for the exploration of these problems are close at hand. The only thing lacking in the shockwave problems is a simple model example like the Galton Board[11] and the conducting oscillator studied here.

VII. ACKNOWLEDGMENT

We thank John Ramshaw (Lawrence Livermore National Laboratory) for a continuing series of thought-provoking emails and for sharing his recent work describing the canonical thermostating of dynamical systems in very general terms[20].

---

[1] S. Nosé, "A Molecular Dynamics Method for Simulations in the Canonical Ensemble", Molecular Physics **52**, 255-268 (1984).

[2] S. Nosé, "A Unified Formulation of the Constant Temperature Molecular Dynamics Methods", Journal of Chemical Physics **81**, 511-519 (1984).

[3] W. G. Hoover, "Canonical Dynamics: Equilibrium Phase-Space Distributions", Physical Review A **31**, 1695-1697 (1985).

[4] W. G. Hoover, "Mécanique de Nonéquilibre à la Californienne", Physica A **240**, 1-11 (1997).

[5] G. J. Martyna, M. L. Klein, and M. Tuckerman, "Nosé-Hoover Chains: the Canonical Ensemble *via* Continuous Dynamics", The Journal of Chemical Physics **97**, 2635-2643 (1992).

[6] N. Ju and A. Bulgac, "Finite-Temperature Properties of Sodium Clusters", Physical Review B **48**, 2721-2732 (1993).

[7] W. G. Hoover and B. L. Holian, "Kinetic Moments Method for the Canonical Ensemble Distribution", Physics Letters A **211**, 253-257 (1996).

[8] W. G. Hoover, J. C. Sprott, and P. K. Patra, "Deterministic Time-Reversible Thermostats : Chaos, Ergodicity, and the Zeroth Law of Thermodynamics", Molecular Physics **113**, 2863-2872 (2015) = arXiv 1501.03875.

[9] A. Bulgac and D. Kusnezov, "Canonical Ensemble Averages from Pseudomicrocanonical Dynamics", Physical Review A **42**, 5045-5048 (1990).

[10] D. Kusnezov, A. Bulgac, and W. Bauer, "Canonical Ensembles from Chaos", Annals of Physics **204**, 155-185 (1990) and **214**, 180-218 (1992).

[11] W. G. Hoover, C. G. Hoover, and J. C. Sprott, "Hard Disks and Harmonic Oscillators Near and Far From Equilibrium", Molecular Simulation (in press, 2015) = arXiv 1507.08302.

[12] W. G. Hoover, J. C. Sprott, and C. G. Hoover, "Ergodicity of a Singly-Thermostated Harmonic Oscillator", Communications in Nonlinear Science and Numerical Simulation **32**, 234-240 (2016)

= arXiv 1504.07654.

[13] W. G. Hoover, J. C. Sprott, and P. K. Patra, "Ergodic Time-Reversible Chaos for Gibbs' Canonical Oscillator", Physics Letters A **379**, 2935-2940 (2015) = arXiv 1503.06749.

[14] W. G. Hoover and C. G. Hoover, "Comparison of Very Smooth Cell-Model Trajectories Using Five Symplectic and Two Runge-Kutta Integrators", Communications in Science and Technology **23**, 109-116 (2015) = arXiv 1504.00620.

[15] D. Daems and G. Nicolis, "Entropy Production and Phase-Space Volume Contraction", Physical Review E **59**, 4000-4006 (1999).

[16] H. van Beijeren and J. R. Dorfman, "On Thermostats and Entropy Production", Physica A **279** 32-29 (2000) = arXiv 0006046.

[17] E. G. D. Cohen and L. Rondoni, "Note on Phase-Space Contraction and Entropy Production in Thermostated Hamiltonian Systems", Chaos **8**, 357-365 (1998) = arXiv 9712213.

[18] Wm. G. Hoover, C. G. Hoover, F. J. Uribe, "Flexible Macroscopic Models for Dense-Fluid Shockwaves: Partitioning Heat and Work; Delaying Stress and Heat Flux; Two-Temperature Thermal Relaxation", Proceedings of Advanced Problems in Mechanics (1-5 July 2010), sponsored by the Institute for Problems in Mechanical Engineering under the patronage of the Russian Academy of Sciences = arXiv 1005.1525.

[19] O. G. Jepps and, L. Rondoni, "Deterministic Thermostats, Theories of Nonequilibrium Systems and Parallels with the Ergodic Condition", Journal of Physics **43**, 1-42 (2010).

[20] J. D. Ramshaw, "A General Formalism for Singly-Thermostated Hamiltonian Dynamics", Physical Review E (in press, 2015).